Treatment Planning Optimisation of Modulated Arc Therapy with Burst Mode

Jaimie Alice McGlashan
Supervisors: Dr. Vicky Mak-Hau & Dr. Kerem Akartunali
Deakin University

February 2014

Contents

Postal Address: 111 Barry Street
c/- The University of Melbourne
Victoria 3010 Australia

Email: enquiries@amsi.org.au
Phone: +61 3 8344 1777
Fax: +61 3 9349 4106
Web: www.amsi.org.au

1 Background

Radiotherapy has emerged to become one of the most commonly performed methods used to treat cancer, the leading cause of death worldwide (World Health Organisation, 2014). A typical session involves high-intensity radiation beams being directed at a tumour at various angles or control points from a rotating gantry. The mARC gantry is capable of rotating around a patient's body by 357 degrees partitioned into equally spaced intervals, with the middle point of each interval referred to as a"control point" (CP). At the head of the gantry, a multi-leaf collimator (MLC) is present to create a variety of shapes for the beam to pass through. The shapes are created by forming an opening in the MLC by the horizontal migration of left and right rows of metal leaves. Modulated Arc Therapy (mARC) is a relatively new form of radiotherapy that aims to successfully shrink and eliminate cancer cells, while also sparing the critical organs and tissues that surround the tumour. mARC differs from other forms of radiotherapy, such as intensity modulated radiation therapy (IMRT) in that sessions for mARC typically last 2-3 minutes rather than 15-20 minutes. It differs from volumetric modulated arc therapy (VMAT) in that the beam of radiation is active strictly at the desired control points only. Furthermore, the MLC shape composition is static during the movement to and from control points. These variations, although minor, alter the underlying optimization problem quite significantly. The accuracy of a radiotherapy plan is crucial, hence that the optimisation of it is quite widely studied. Optimisation of VMAT plans, for example, has been recently considered by a number of authors. A multicriteria optimisation has been very recently invesitiaged by Chen *et al.* (2014). Men *et al.* (2010) published an ultra fast approach the planning. Heuristic approaches to the treatment plan optimisation were presented by Akartunali and Mak (2012). As mARC is a new form of treatment, limited studies on its optimisation have been conducted thus far.

Figure 1: A photo of the machinery utilised during a typical radiotherapy session. (Photo courtesy of the ALCC, Barwon Health)

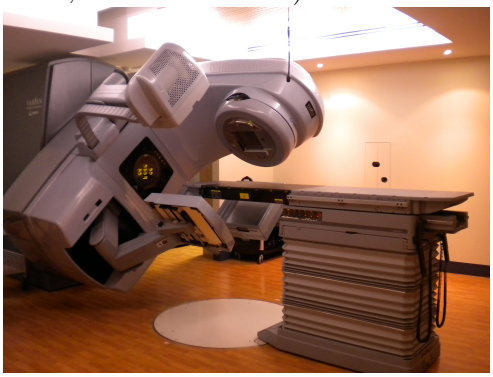

Figure 2: A visual representation of the MLC machinery and functionality. (Photo courtesy of the ALCC, Barwon Health)

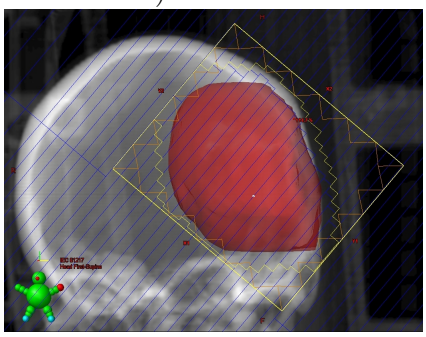

2 Aims

In this project, we aim to study the treatment planning optimisation of mARC. To achieve this, two mixed-integer linear programming models will be developed and compared. Although each patient's case is different, the fundamental objective of the model is to maximize the dose delivered to the tumour whilst sparing nearby organs at risk (OAR). The output of the optimisation will present the control points where radiation beams are active and the intensity delivered from each. Results obtained will obey a number of mARC machinery and prescribed dosage constraints. We will experiment the MILPs on small-scale test problems to examine the differences in computation time for each.

3 Model Formulation

Two models have been constructed to optimise mARC plans. The first is based on the VMAT treatment planning optimisation from Akaratunali and Mak (2012) where a MILP is presented. The second model breaks down a relatively complex variable $y^k_{i(\ell,r)}$ into three separate variables, as seen in the VMAT model published by Sun *et al.* (2013) and by Langer *et al.* (2001) for an IMRT model. The motivation for constructing two models is to undertake an analysis on the computation times for each, as minimising planning time is imperative.

3.1 Objective Functions

An optimisation model always contains an objective function to be maximised or minimised. In the case of radiotherapy, the objective functions to choose range from minimising treatment time, maximising dose to tumour or minimising radiation delivered to OAR. For our project, we have adopted the objective of maximising the number of voxels in a tumour that receive at least their desired dose.

3.2 Model 1 Variables and Parameters

We first define a number of variables and parameters which we use in our mathematical model. We define:

- $\mathcal{K}$, the index set of all control points;
- $\mathcal{L} = \{(\ell, r) \mid \ell, r \in \mathcal{N}, \ell < r\}$ be the feasible left and right-leaf pairs;
- $\mathcal{M}$, the index set of the rows of an MLC, and $m = |\mathcal{M}|$;
- $\mathcal{N}$, the index set of assumed columns an MLC is partitioned into, and $n = |\mathcal{N}|$;
- $\alpha_k \in \{0, 1\}$ to be a binary variable with $\alpha_k = 1$ indicating radiation is delivered in CP k;
- $\bar{\alpha}$, the maximum number of consecutive active CPs (the maximum alpha angle);
- $\underline{\beta}$, the minimum size of separation of CPs in units of intervals;
- $\mathcal{T}$ the set of all voxels in Planning Target Volumes (PTV);
- $\mathcal{O}$ the set of all voxels in Organs At Risk (OAR);

- U_v the upper bound on radiation that is delivered to voxel $v \in \mathcal{O}$;
- L_v the lower bound on radiation that should be delivered to voxel $v \in \mathcal{T}$;
- $D^k_{i,j,v}$ a parameter which indicates the intensity per unit radiation delivered from Row i and Column j of CP k to voxel v;
- $y^k_{i(\ell,r)} \in \{0,1\}$ to be a decision variable with $y^k_{i(\ell,r)} = 1$ if the bixels between, but not including, columns ℓ and r in row i in Snapshot k are open and $y^k_{i(\ell,r)} = 0$ otherwise;
- $x_v \in \{0,1\}$ a decision variable with $x_v = 1$ if voxel $v \in \mathcal{T}$ receives a desired dose of $\bar{d}$ or above and $x_v = 0$ otherwise.
- d_v the dose that voxel v receives; and
- z^k a continuous decision variable representing the monitor units or fluence weights for snapshot k.

3.3 Model 2 Variables and Parameters

Model 2 differs only slightly from Model 1 in they way how leaf positions are represented.

- t^k_{ij} be a binary variable with $t^k_{ij} = 1$ if bixel i,j in snapshot k is open, and $t^k_{ij} = 0$ otherwise.
- ℓ^k_{ij} be a binary variable with $\ell^k_{ij} = 1$ indicating the column j in row i of snapshot k is closed by the left leaf and $\ell^k_{ij} = 0$ otherwise; and
- r^k_{ij} be a binary variable with $r^k_{ij} = 1$ indicating the column j in row i of snapshot k is closed by the right leaf and $r^k_{ij} = 0$ otherwise.

These variables are inspried from Langer *et al.* 2001 for IMRT and in Sun *et al.* 2013 for VMAT.

3.4 The Optimisation Model

We start with the objective function.

$$max \sum_{v \in T} x_v \tag{1}$$

3.4.1 mARC Machinery Constraints

We first present constraints for modelling the machinery restrictions of the mARC. They ensure that the maximum alpha angle is no more than $\bar{\alpha}$ units and that the minimum separation between two active control points, $\underline{\beta}$ is observed.

$$\sum_{\delta=0}^{\bar{\alpha}} \alpha_{k+\delta} \leq \bar{\alpha}, \quad \forall k = 1, \ldots, |\mathcal{K}| - \bar{\alpha}. \tag{2}$$

for all $k = 1, \ldots, |\mathcal{K}| - \underline{\beta} - 1$, if $\alpha_k - \alpha_{k+1} = 1$, then

$$\sum_{\delta=1}^{\underline{\beta}} (1 - \alpha_{k+\delta}) = \underline{\beta}, \quad \forall k = 1, \ldots, |\mathcal{K}| - \underline{\beta} - 1. \tag{3}$$

$$\sum_{\delta=1}^{\underline{\beta}} (1 - \alpha_{k+\delta}) \geq \underline{\beta}\ (\alpha_k - \alpha_{k+1}), \quad \forall k = 1, \ldots, |K| - \underline{\beta} - 1. \tag{4}$$

These constraints are valid for both models.

3.4.2 MLC Leaf-pair Constraints

Models 1 and 2 require individual formulation of MLC leaf-pair constraints.

Model 1.

$$\sum_{(\ell,r) \in \mathcal{L}} y^k_{i(\ell,r)} = 1, \quad \forall i \in \mathcal{M},\ \forall k \in \mathcal{K}. \tag{5}$$

Model 2.

$$t^k_{ij} + \ell^k_{ij} + r^k_{ij} = 1, \forall i \in \mathcal{M},\ j \in \mathcal{N},\ k \in \mathcal{K} \tag{6}$$

$$r^k_{i,j} \leq r^k_{i,j+1}, \forall i \in \mathcal{M},\ j \in \mathcal{N} \setminus \{1\}\ k \in \mathcal{K} \tag{7}$$

$$\ell^k_{i,j} \geq \ell^k_{i,j+1}, \forall i \in \mathcal{M},\ j \in \mathcal{N} \setminus \{1\}\ k \in \mathcal{K} \tag{8}$$

Postal Address: 111 Barry Street
c/- The University of Melbourne
Victoria 3010 Australia

Email: enquiries@amsi.org.au
Phone: +61 3 8344 1777
Fax: +61 3 9349 4106
Web: www.amsi.org.au

3.4.3 MLC Interleaf Constraints

Next we require that the left leaf of any row can not collide with the right leaf of the adjacent rows, and vice versa. To monitor this, we use the following constraints.

Model 1.

$$\sum_{\tilde{r}=\ell+1}^{n+1} y^k_{i(\ell,\tilde{r})} + \sum_{\tilde{r}=1}^{\ell}\sum_{\tilde{\ell}=0}^{\tilde{r}-1} y^k_{(i+1)(\tilde{\ell},\tilde{r})} \leq 1 \quad \forall i \in \mathcal{M}\setminus\{m\}, \forall \ell \in \mathcal{L}\cup\{0\}, \forall k \in \mathcal{K}. \tag{9}$$

$$\sum_{\tilde{\ell}=0}^{r-1} y^k_{i(\tilde{\ell},r)} + \sum_{\tilde{\ell}=r}^{n}\sum_{\tilde{r}=\tilde{\ell}+1}^{n+1} y^k_{(i+1)(\tilde{\ell},\tilde{r})} \leq 1 \quad \forall i \in \mathcal{M}\setminus\{m\}, \forall r \in \mathcal{L}\cup\{n+1\}, \forall k \in \mathcal{K}. \tag{10}$$

Model 2.

$$r^k_{i,j} + l^k_{i+1,j} \leq 1, \quad ,\forall j \in J,\ k \in K, \forall i \in \mathcal{M}\setminus\{1\} \tag{11}$$

$$r^k_{i+1,j} + l^k_{i,j} \leq 1, \quad ,\forall j \in J,\ k \in K \forall i \in \mathcal{M}\setminus\{1\} \tag{12}$$

These constraints are presented in Langer *et al.* 2001 for IMRT treatment planning optimisation.

3.4.4 'Linking' constraints

To tie the MLC aperture variables and the fluence weight variables at each control point with the α variables, we require that:

1. If $\alpha_k = 0$, then $z^k = 0$, for all $k \in \mathcal{K}$.
2. For each $k = 1, \ldots, |\mathcal{K}| - 1$, if $\alpha_k = \alpha_{k+1} = 1$, then $y^k_{i(\ell,r)} = y^{k+1}_{i(\ell,r)}$, for all $i \in \mathcal{M}$, $j \in \mathcal{N}$; and $z^k = z^{k+1}$ for model 1.
3. For each $k = 1, \ldots, |\mathcal{K}| - 1$, if $\alpha_k = \alpha_{k+1} = 1$, then $t^k_{ij} = t^{k+1}_{ij}$, for all $i \in \mathcal{M}$, $j \in \mathcal{N}$; and $z^k = z^{k+1}$ for model 2.

To acheive this, we introduce a new variable s_k. Let s_k be binary variable indicating whether $\alpha_k = \alpha_{k+1} = 1$ (i.e., two consecutive control points are part of an opening and

hence should be consistent, $s_k = 1$) or not ($s_k = 0$).

$$\begin{aligned}
\alpha_k + \alpha_{k+1} - 1 &\leq s_k, \quad \forall k \in K \\
\alpha_k &\geq s_k, \quad \forall k \in K \\
\alpha_{k+1} &\geq s_k, \quad \forall k \in K \\
s_k - 1 \leq y^k_{i(\ell,r)} - y^{k+1}_{i(\ell,r)} &\leq 1 - s_k, \quad \forall k \in K,\ i \in \mathcal{M}, j \in \mathcal{N} \\
\bar{\mathcal{W}}(s_k - 1) \leq z^k - z^{k+1} &\leq \bar{\mathcal{W}}(1 - s_k), \quad \forall k \in K
\end{aligned}$$

Note that for Model 2: $y^k_{i(\ell,r)}$ is replaced by t^k_{ij}.

3.4.5 Dose Limit Constraints

To ensure that the lower and upper dosage limits are satisfied, we have that:

$$d_v \geq L_v \quad v \in V_t \tag{13}$$

$$d_v \leq U_v \quad v \in V \tag{14}$$

$$d_v - L_v \geq (\bar{d} - L_v)x_v \quad v \in V_t \tag{15}$$

3.4.6 Dose Calculation

The dose received by a voxel, d_v for all $v \in V$ is dependent on the MU delivered and the shape of the MLC at each snapshot. It's value is calculated as follows:

$$d_v = \sum_{k \in \mathcal{K}} \sum_{i \in \mathcal{M}} \sum_{j \in \mathcal{N}} \left(z^k \times D^k_{ijv} \times \sum_{(\ell,r) \in \mathcal{L}} y^k_{i(\ell,r)} \right) \tag{16}$$

Note again, for model 2: $y^k_{i(\ell,r)}$ is replaced by t^k_{ij} for the dosage calculation.

To linearise the above, we introduce a variable, $\bar{z}^k_{ij}$ to represent the MU amount, (or fluenceweight) for beamlet (i, j) from snapshot k. Hence producing the following linear calculation fo d_v.

$$d_v = \sum_{k\in\mathcal{K}} \sum_{i\in\mathcal{M}} \sum_{j\in\mathcal{N}} \left(\bar{z}^k_{ij} \times D^k_{ijv}\right) \tag{17}$$

Lastly, to finalise the linearisation we have the following four constraints:

Model 1.

$$\bar{z}^k_{ij} \leq \bar{M} \sum_{(\ell,r)\in\mathcal{L},,\ell<j<r} y^k_{i(\ell,r)} \tag{18}$$

$$\bar{z}^k_{ij} \leq z^k \tag{19}$$

$$\bar{z}^k_{ij} \geq \bar{M}(-1 + \sum_{(\ell,r)\in\mathcal{L},\ell<j<r} y^k_{i(\ell,r)} + z^k) \tag{20}$$

$$\bar{z}^k_{ij} \geq 0 \tag{21}$$

Model 2.

$$\bar{z}^k_{ij} \leq \bar{M} t^k_{ij} \tag{22}$$

$$\bar{z}^k_{ij} \leq z^k \tag{23}$$

$$\bar{z}^k_{ij} \geq \bar{M}(-1 + t^k_{ij}) + z^k \tag{24}$$

$$\bar{z}^k_{ij} \geq 0 \tag{25}$$

4 Numerical Results

Here we present the numerical results obtained from our experiment. The models were both tested on 4 problem instances. Three simple instances (a, b and c) containing 4 snapshots and one larger instance with 90 snapshots (d). The data instances were randomly generated using a random problem generate code written in C++. Fig 3 shows MLC shapes as determined by a random instance. Table 1 presents the values of some decision variables obtained from one of the small sets, data instance (b). The parameters for the data sets are as follows:
(a, b, c): Snapshots = 4; Rows = 4; Columns = 4; w = h = d = 4; $\bar{\alpha}$=2; $\underline{\beta}$=1.
(d): Snapshots = 90; Rows = 6; Columns = 6; w = h = d = 6; $\bar{\alpha}$=3; $\underline{\beta}$=2.

Table 1: The objective value, a_k and z_k values for a 4 snapshot data set (instance b).

Objective	3
a_k	[1, 0, 1, 0]
z_k	[1.3946, 0, 1.427, 0]

Figure 3: The optimised MLC shapes for each snapshot in a random 4 snapshot sample.

Instance No.	Model 1 time (mins)	Model 2 time (mins)
(a)	00:09:97	00:02:52
(b)	00:14:43	00:01:99
(c)	00:14:79	00:03:77
(d)	46:47:67	05:32:44

Table 2: A comparison of completion time among the two models for the 4 instances.

As suggested by the results in Table 2, the alteration of the original MLC shape variable, $y^k_{i(\ell,r)}$ to the three variables in Model 2 has resulted in significanty shorter computation time. Given that one of the main advantages of mARC is the extremely fast sessions, it is ideal to aim for quick treatment planning too.

5 Conclusion

Optimisation models were written to find optimal control points, intensities and MLC shapes that obey machinery and dosage constraints. By creating two models, we could conduct an analysis as to which is the most desirable time wise.

5.1 Future Direction

As this project is continued as an Honours project in 2014 at Deakin University, projected direction for the year includes further study of relaxations, solution methods and advanced programming. Although we reduced computation time by constructing Model 2 in this research, further implementations will be investigated to continue to shorten time. Finally, I hope to test the optimisation model on some real-life large-scale problems.

5.2 Acknowledgements

A big thank you to AMSI, CSIRO and Vicky for an excellent experience.

References

[1] Akartunali, K. and Mak-Hau, V. (2012) *Treatment Planning Optimization for Volumetric-Modulated Arc Therapy* Technical Report, University of Strathclyde and Deakin University.

[2] Chen, H., Craft, D. L., and Gierga, D. P. (2014). *Multicriteria optimization informed VMAT planning.* Medical Dosimetry,39(1), 64-73. doi:10.1016/j.meddos.2013.10.001

[3] Dzierma, Y., Nuesken, F., Licht, N., and Ruebe, C. (2013). *A novel implementation of mARC treatment for non-dedicated planning systems using converted IMRT plans.* Radiation Oncology (London, England), 8(1), 193.

[4] Langer, M., Thai, V., and Papiez, L. (2001). *Improved leaf sequencing reduces segments or monitor units needed to deliver IMRT using multileaf collimators.* Medical Physics, 28(12), 2450-2458.

[5] Men, C., Romeijn, H., Jia, X., and Jiang, S. (2010). *Ultrafast treatment plan optimization for volumetric modulated arc therapy (VMAT).* Medical Physics, 37(11), 5787-5791. DOI: 10.1109/IPDPS. 5470444.

[6] World Health Organisation. (2014, February). *Cancer*. Retrieved from World Health Organisation: http://www.who.int/mediacentre/factsheets/fs297/en/